

This is an author produced version of a paper published in  
Carbohydrate polymers.

This paper has been peer-reviewed and is proof-corrected, but does not  
include the journal pagination.

Citation for the published paper:

Menzel, Carolin; Andersson, Mariette; Andersson, Roger; Vazquez-  
Gutierrez, Jose L.; Daniel, Geoffrey; Langton, Maud; Gällstedt, Mikael;  
Koch, Kristine. (2015) Improved material properties of solution-cast starch  
films: Effect of varying amylopectin structure and amylose content of starch  
from genetically modified potatoes. *Carbohydrate polymers*. Volume: 130,  
pp 388-397.

<http://dx.doi.org/10.1016/j.carbpol.2015.05.024>.

Access to the published version may require journal subscription.

Published with permission from: Elsevier.

Standard set statement from the publisher:

© Elsevier, 2016 This manuscript version is made available under the CC-BY-NC-ND 4.0  
license <http://creativecommons.org/licenses/by-nc-nd/4.0/>

Epsilon Open Archive <http://epsilon.slu.se>

1 Improved material properties of solution cast starch  
2 films: effect of varying amylopectin structure and  
3 amylose content of starch from genetically modified  
4 potatoes

5 *CAROLIN MENZEL<sup>1\*</sup>, MARIETTE ANDERSSON<sup>2</sup>, ROGER ANDERSSON<sup>1</sup>, JOSÉ L.*  
6 *VÁZQUEZ-GUTIÉRREZ<sup>1</sup>, GEOFFREY DANIEL<sup>3</sup>, MAUD LANGTON<sup>1</sup>, MIKAEL GÄLLSTEDT<sup>4</sup>,*  
7 *KRISTINE KOCH<sup>1</sup>*

8 <sup>1</sup> Department of Food Science, Swedish University of Agricultural Sciences, Box 7051, SE-750  
9 07 Uppsala, Sweden

10 <sup>2</sup> Department of Plant Breeding, Swedish University of Agricultural Sciences, Box 101, SE-230  
11 53 Alnarp, Sweden

12 <sup>3</sup> Department of Forest Products, Swedish University of Agricultural Sciences, Box 7008, SE-  
13 750 07 Uppsala, Sweden

14 <sup>4</sup> Innventia AB, Box 5604, SE-114 86 Stockholm, Sweden

15 **Corresponding Author**

16 \*Carolín Menzel, phone: +46 1867 2070, fax: +46 1867 2995, e-mail: carolin.menzel@slu.se

17 Department of Food Science, Swedish University of Agricultural Sciences, Box 7051, SE-750 07  
18 Uppsala, Sweden

19 ABSTRACT

20 High-amylose potato starches were produced through genetic modification resulting in changed  
21 granule morphology and composition with higher amylose content and increased chain-length of  
22 amylopectin. The increased amylose content and structural changes in amylopectin gave  
23 improved film forming behavior and better barrier and tensile properties in starch films. The  
24 molecular structure in these starches was related to film-forming properties. Solution-cast films  
25 of high-amylose starch revealed a homogeneous structure with increasing surface roughness at  
26 higher amylose content, possibly due to amylose aggregation. Films exhibited significant higher  
27 stress and strain at break compared to films of wild-type starch, which could be attributable to  
28 the longer chains of amylopectin being involved in the interconnected network and more  
29 interaction between chains as shown using transmission electron microscopy. The oxygen  
30 permeability of high-amylose starch films was significantly decreased compared to wild-type  
31 starch. The nature of the modified starches makes them an interesting candidate for replacement  
32 of non-renewable oxygen and grease barrier polymers used today.

33 KEYWORDS

34 high-amylose potato starch, film forming, molecular structure, chain-length, amylopectin,  
35 microscopy

## 36 **1. Introduction**

37 Starch is well known for its excellent film forming and oxygen barriers capabilities and thus a  
38 potential replacement of synthetic polymers in food packaging. Starch consists of two major  
39 components, mainly linear amylose and branched amylopectin, both of which consist of glucose  
40 residues but differ in physicochemical properties. Already in the early 1950s much attention was  
41 given to amylose starches because of their good film-forming properties and their manifold of  
42 applications (Wolff, Davis, Cluskey, Gundrum & Rist, 1951). Amylose is used in coatings of  
43 food products, sweets or fibre-fortified foods, and as gelling agent because of its ability to create  
44 high-strength gels, e.g. to enhance the structure of food products such as tomato paste  
45 (Richardson, Jeffcoat & Shi, 2000; Van Patten & Freck, 1973). There have been many attempts  
46 to use high-amylose starches in, e.g. composites together with waxes (Muscat, Adhikari,  
47 McKnight, Guo & Adhikari, 2013) or chitosan (Feng, Hu & Qiu, 2013) or were extruded (Li et  
48 al., 2011) and plasticized together with glycerol (Muscat, Adhikari, Adhikari & Chaudhary,  
49 2012) to produce packaging material from natural resources. Since amylose consists mainly of  
50 linear chains, a tight and stable network with strong molecular orientation can be created in films  
51 (Rindlav-Westling, Stading, Hermansson & Gatenholm, 1998). Amylose films are capable of  
52 being greaseproof (Banks, Greenwood & Muir, 1974) and have been shown to perform better in  
53 terms of mechanical and oxygen barrier properties than amylopectin films (Liu, 2005; Lourdin,  
54 Valle & Colonna, 1995; Myllarinen, Partanen, Seppala & Forssell, 2002; Rankin, Wolff, Davis  
55 & Rist, 1958; Rindlav-Westling, Stading, Hermansson & Gatenholm, 1998). Hence, there have  
56 been several efforts to find natural mutants or to develop crops with high-amylose starch in  
57 tubers and grains which would be beneficial from a techno-functional point of view (Banks,  
58 Greenwood & Muir, 1974; Walker & Merritt, 1969; Wolff, Hofreiter, Watson, Deatherage &

59 MacMasters, 1955). Extensive amylose breeding programs, such as that by National Starch  
60 (Forsyth, IL., USA) have resulted in commercial crops with up to 90% amylose (Sidebottom,  
61 Kirkland, Strongitharm & Jeffcoat, 1998). However, in many plants, for example potato, no  
62 natural mutants have been described and genetic modification has been used to introduce the  
63 high-amylose trait. Starches from potato have a distinctive quality, with a high amount of  
64 phosphate and low content of lipids, which is beneficial for many applications where good  
65 clarity, neutral taste or high swelling is needed. They are therefore of considerable industrial  
66 interest and potato is an important target crop for modified starch qualities (Zeeman, Kossmann  
67 & Smith, 2010). In potato breeding studies, intense focus has been placed on modifying the  
68 expression of enzymes involved in the synthesis of amylose and amylopectin to change the  
69 starch structure. Schwall et al. (2000) down-regulated two starch branching enzymes, *SBE A* and  
70 *SBE B*, resulting in high-amylose producing potatoes (Schwall et al., 2000). These starches  
71 exhibited up to 56% amylose, a low amount of high molecular weight ( $M_w$ ) amylopectin and an  
72 increased number of long chains in starch which may represent an amylose population with long-  
73 branches which is normally minor in starch.. Hofvander and coworkers (2004) also produced  
74 several high-amylose starches from four potato cultivars with amylose contents ranging between  
75 40 and 86%, the starch with the highest amylose content also having a low degree of branching  
76 (0.31%) compared with wild-type potato (about 2.3%) (Hofvander, Andersson, Larsson &  
77 Larsson, 2004). In earlier studies on high-amylose maize starches, amylose fractions appeared to  
78 be unaffected in structure in all aspects except the average  $M_w$  (Banks, Greenwood & Muir,  
79 1974). However, the amylopectin fraction of these starches differed in structure, showing greater  
80 average chain length, higher beta-limit values and higher retrogradation tendency in concentrated  
81 solution (Banks, Greenwood & Muir, 1974).

82 It has been shown that commercially available amylose in a mixture with amylopectin exhibits  
83 different physicochemical properties from wild-type starches with the same  
84 amylose/ amylopectin ratio. It has also been reported that purified amylose added to starch had a  
85 higher crystallinity than predicted from wild-type starch probably due to lower  $M_w$  (Rindlav-  
86 Westling, Stading & Gatenholm, 2001). In addition, it is known that  $M_w$  influences the  
87 mechanical properties (Lourdin, Valle & Colonna, 1995; Wolff, Davis, Cluskey, Gundrum &  
88 Rist, 1951). However, not only the effect of high amylose content or high  $M_w$  but also structural  
89 differences in amylose and amylopectin molecules might give different network microstructure  
90 and influence mechanical and barrier properties.

91 In this study, starches with different amounts of amylose from three genetically modified potato  
92 lines were characterized in order to understand the interrelation between molecular structure and  
93 physical properties and predict the properties of these starches in materials such as films and  
94 coatings. All three high-amylose starches were used to prepare solution-cast films to examine  
95 their film-forming ability and their physical properties, i.e. barrier and tensile properties.  
96 Different microscopy techniques were used to study the microstructure of the starches and films.  
97 Properties of films were correlated to their microstructure and possible applications are  
98 discussed.

99

## 100 **2. Materials and methods**

### 101 **2.1 Materials**

#### 102 *Development and growth of high-amylose potato lines*

103 High amylose potato lines were generated essentially as described previously (Andersson,  
104 Melander, Pojmark, Larsson, Bulow & Hofvander, 2006). In brief, 200 bp of two starch  
105 branching enzymes, *SBE1* and *SBE2*, were synthetically produced in tandem (Eurofins  
106 Genomics, Ebersberg, Germany), flanked by *attB* sites, and cloned into the binary vector  
107 pGWIWgbss via pDonor221 using the Gateway® system (Invitrogen, Carlsbad, CA, USA).  
108 pGWIWgbss is a modified version of the pK7GWIWG2(II) (Karimi, Inze & Depicker, 2002)  
109 vector, in which the 35S promoter has been replaced by a granular bound starch synthase  
110 (*GBSS*) promoter of *Solanum tuberosum* origin. Three potato cultivars, Kuras, Verba and  
111 Dinamo, were transformed using *Agrobacterium tumefaciens* strain AGLO harboring the RNAi  
112 construct. Transformation, regeneration and selection of lines were performed as described by  
113 Andersson et al. (2006) with the modification that 50 mg/ L kanamycin was used as the selection  
114 agent (Andersson, Trifonova, Andersson, Johansson, Bulow & Hofvander, 2003). High-amylose  
115 lines were grown in the greenhouse with 16 hours day length, 18/15 °C day/night temperature  
116 and 75% relative humidity for 5 months. Starch was extracted from mature tubers using a  
117 protocol described elsewhere (Larsson, Hofvander, Khoshnoodi, Ek, Rask & Larsson, 1996). In  
118 brief, tubers were peeled and homogenized at 4 °C with a fruit juicer. Tris-HCl (pH 7.5, 50 mM),  
119 Na-dithionite (30 mM) and EDTA (10 mM) was added and starch granules were allowed to  
120 sediment and washed four times with buffer and three times with acetone before drying  
121 overnight at room temperature.

### 122 **2.2 Methods**

123 *2.2.1 Light microscopy for characterization of starch granule shape and size*

124 Size and shape of starch granules were determined using a light microscope (Nikon Eclipse Ni-U  
125 microscope, Tokyo, Japan) and images were captured with a Nikon DS-Fi2-U3 Camera (Nikon  
126 Corporation, Japan). Polarized light was used to show crystallinity and iodine staining to detect  
127 amylose using 100 mg starch dispersed in 2 mL water and 50 $\mu$ L Lugol's solution (1g KI + 0.1g  
128 I<sub>2</sub> in 50mL water).

129

130 *2.2.2 Starch content determination with thermostable  $\alpha$ -amylase*

131 The purity of the starch was determined enzymatically as described elsewhere (Åman,  
132 Westerlund & Theander, 1994). In brief, starch was treated with thermostable  $\alpha$ -amylase (EC  
133 3.2.1.1; 3000 U/mL; Megazyme, Wicklow, Ireland) in a boiling water bath for 30 min.  
134 Afterwards an amyloglucosidase (EC 3.2.1.3, 260 U/mL, Megazyme, Wicklow, Ireland )  
135 solution was added and the sample allowed to stand overnight in a 60 °C water bath. At the next  
136 day, GOPOD reagent (Glucose oxidase plus peroxidase and 4-aminoantipyrine, Megazyme,  
137 Wicklow, Ireland) was added and absorbance measured at 510 nm. Starch content was calculated  
138 in terms of glucose concentration using a two-point calibration with a D-glucose standard (ready  
139 to use solution from Megazyme). All chemicals used were of analytical grade.

140

141 *2.2.3 Amylose content in modified and wild-type starches*

142 The amount of amylose was measured colorimetrically using the iodine complex formation  
143 method described elsewhere (Chrastil, 1987). Calibration of amylose content was performed on  
144 different mixtures of potato amylose standard (type III, Sigma Chemical CO., MO, USA) and

145 granular potato amylopectin starch (Lyckeby Starch AB, Kristianstad, Sweden) with  
146 concentrations of amylose from 10-70% ( $R^2=0.972$ ).

147

#### 148 *2.2.4 Separation of amylose and amylopectin*

149 To study the fine structure of high-amylose starches, amylose and amylopectin were isolated  
150 according to Klucinec and Thompson (1998) with minor modifications (Klucinec & Thompson,  
151 1998). About 2 g starch were dissolved in 56 mL 90% DMSO at 90 °C under nitrogen stream. A  
152 mixture of n-butanol:isoamyl alcohol:water (372 mL; 23.5:23.5:325; v:v:v) was added drop-wise  
153 at 80 °C under nitrogen stream (ca 1.5 h) and the sample slowly cooled to room temperature. The  
154 solution was centrifuged at 13000 g at 4 °C for 2 h. The supernatant with amylopectin was  
155 decanted and the solvent evaporated. The amylopectin and amylose fractions were dissolved  
156 separately in hot water (about 30 mL) and 3 volumes of methanol were added. The solution was  
157 allowed to rest for 1 h at room temperature. Methanol was then decanted after centrifugation  
158 (6600 g, 4 °C and 2 h) and the remaining pellet once more dissolved in hot water (30 mL) and  
159 treated likewise with ethanol (3 volumes). The amylose and amylopectin were freeze-dried and  
160 checked for purity using gel permeation chromatography (GPC; Sepharose CL-6B) after  
161 debranching as described below.

162

#### 163 *2.2.5 Molecular size distribution and amylose content using CL-6B columns after debranching*

164 Size distribution of whole potato starch was measured using GPC on a Sepharose CL-6B column  
165 (90 cm x 1.0 cm) after debranching with isoamylase (glycogen 6-glucohydrolase; EC 3.2.1.68;  
166 from *Pseudomonas* sp.; specific activity 280 U/mg) and pullulanase (amylopectin 6-  
167 glucohydrolase; EC 3.2.1.41; from *Klebsiella planticola*; specific activity 42 U/mg) as

168 described elsewhere (Bertoft & Spoof, 1989). Fractions of 0.5 mL were collected and analyzed  
169 with phenol-H<sub>2</sub>SO<sub>4</sub> reagent (DuBois, Gilles, Hamilton, Rebers & Smith, 1956). Granular potato  
170 amylopectin starch (Lyckeby Starch AB, Kristianstad, Sweden) was used to indicate the elution  
171 volume where chains from amylopectin elute from the column (85 mL) and was used as limit to  
172 calculate amylose content (relative area under the curve eluting before 85 mL). Purity and size  
173 distribution of separated starch components, i.e. amylose and amylopectin, were determined  
174 accordingly.

175

#### 176 *2.2.6 Chain length distribution using high-performance anion-exchange chromatography* 177 *(HPAEC)*

178 Chain length distribution of amylopectin was determined using a Dionex HPAEC system  
179 (Dionex, Sunnyvale, CA, USA) with a CarboPac PA-100 column (4 × 250 mm) coupled with a  
180 pulsed amperometric detector. A gradient of NaOAc in 0.15 M NaOH was used to elute starch  
181 chains, as described in detail elsewhere (Koch, Andersson & Åman, 1998).

182

#### 183 *2.2.7 Pasting properties using rapid visco analysis (RVA)*

184 Starch pasting properties were analyzed using RVA (Newport Scientific, Warriewood, NSW,  
185 Australia). The standard method 1 according to the manufacturer was used, where 25.0 mL water  
186 was added into an aluminum canister and 2.0 g starch (dry weight) was added. The paddle  
187 rotation was kept constant at 160 rpm throughout the analysis. The suspension was equilibrated  
188 at 50 °C for 1 min, heated at a rate of 12.2 K/ min to 95 °C and kept for 3.5 min before cooling to  
189 50 °C at a rate of 11.8 K/ min.

190

191 *2.2.8 Solution-casting of starch films*

192 Aqueous starch solutions (180 mg dry weight/ 6 mL water) were heated to 140 °C in a closed  
193 tube and held for 45 min under permanent stirring in a Pierce Reacti-Therm heating/ stirring  
194 module. The solutions were allowed to cool to around 70 °C and 3.5 mL of the solution were  
195 transferred to a Petri dish (5.5 cm diameter). Bigger Petri dishes (8.5 cm diameter and 8.4 mL  
196 solution) were used to produce films for barrier properties and tensile testing. The solvent was  
197 evaporated at 23 °C overnight and allowed to dry for 48 h.

198

199 *2.2.9 Microstructural study of solution-cast films*

200 Scanning electron microscopy (SEM) was carried out using a Philips XL 30 ESEM operated at  
201 10 kV, to observe the surface of the starch films. Samples were previously gold-coated using an  
202 Emitech K550X sputter device (Quorum Technologies Ltd, Ashford, Kent, UK).

203 For TEM, fragments of approximately 2 mm<sup>2</sup> were cut out of the films and embedded in TAAB  
204 812 resin (epoxy) without prior fixation and dehydration. Thin sections (about 75 nm) were cut  
205 using a diamond knife on a Leica EM UC6 ultramicrotome and collected on gold grids. Sections  
206 were stained according to the periodic acid-thiosemicarbazide-silver proteinate method described  
207 elsewhere (Thiéry, 1967) prior to examination with a Philips CM/12 transmission electron  
208 microscope using an accelerating voltage of 80 kV.

209

210 *2.2.10 Material properties of solution-cast films*

211 Oxygen transmission rate (OTR) was measured in a Mocon Ox-Tran 2/21 (SH) in duplicate  
212 according to standard method ASTM F1927 – 07 and oxygen permeability (OP) was calculated  
213 based on film thickness (measured at six random places within the film). Prior to OTR

214 measurements, samples were conditioned at 23 °C and 50% RH. Tensile testing of starch films  
215 was performed according to ASTM D882-02. Before punching out dumbbell shaped specimens,  
216 samples were kept in an air-conditioned climate chamber at 23 °C and 50% RH.

217 **3. Results and discussion**

218 Three high-amylose potatoes from three cultivars Kuras, Verba and Dinamo were produced by  
219 suppression of the starch branching enzymes *SBE1* and *SBE2* and are denoted LowAm-1068,  
220 MidAm-7040 and HighAm-2012, respectively. All high-amylose lines resulted in higher tuber  
221 yield but lower dry matter which is attributed to lower starch content (Table 1), a feature  
222 reported previously for high-amylose potato lines (Hofvander, Andersson, Larsson & Larsson,  
223 2004). The extracted starch from each potato wild-type cultivar and their high-amylose lines  
224 were characterized in detail and their film-forming ability studied in terms of microstructure and  
225 physical properties.

226

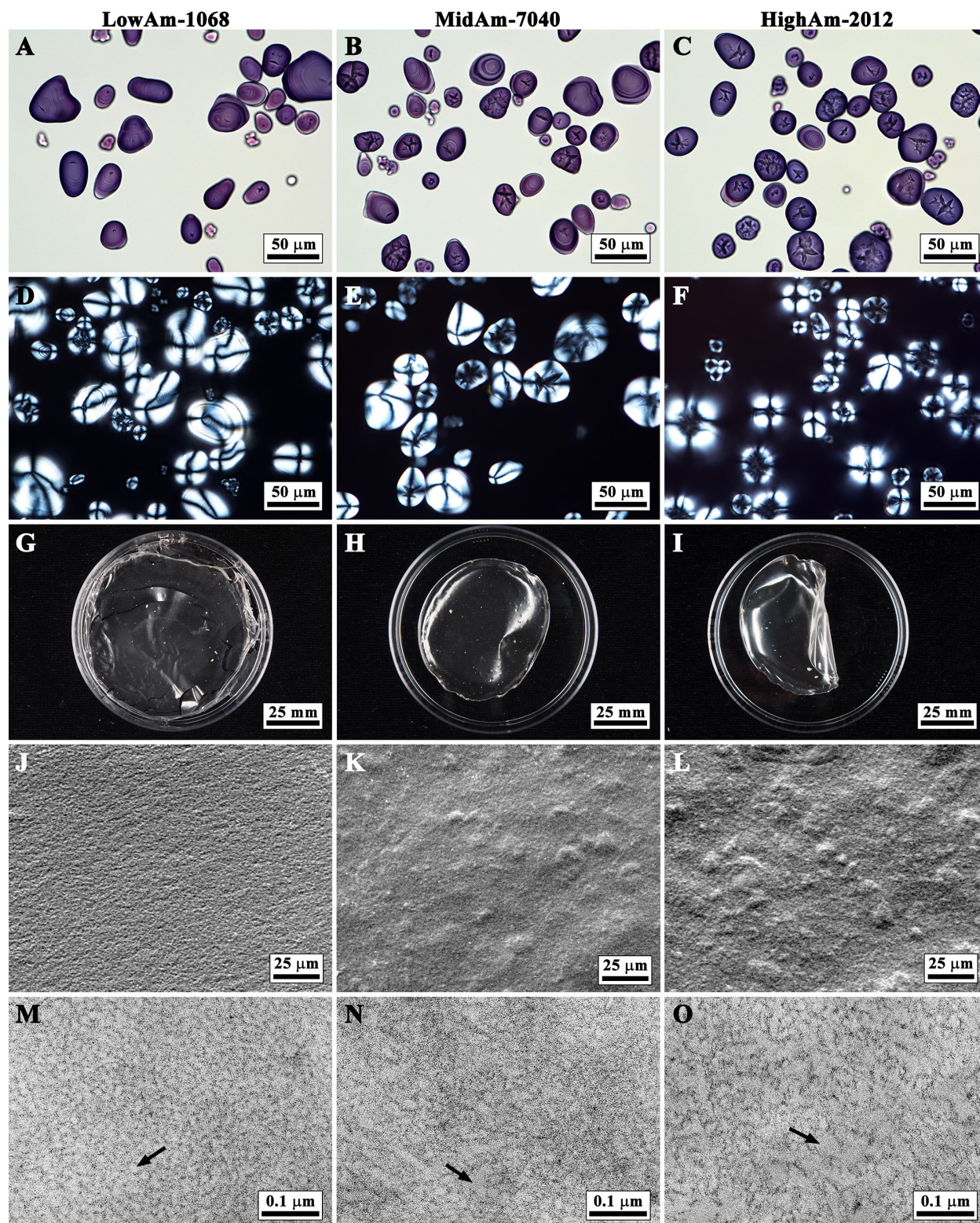
227 **3.1 Light microscopy for morphology and birefringence of starch granules**

228 Starch granules from high-amylose lines exhibited different shapes and sizes compared to wild-  
229 type potato (Figure 1 A-C). Those in wild-type potatoes were typically oval, round or even  
230 irregular shaped (data not shown), whereas with increasing amount of amylose, the starches had  
231 an increasing amount of very small, rod-shaped granules which did not exist in wild-type  
232 starches. Also, starch granules of high-amylose lines showed fissures in the middle of the  
233 granules. This has been reported before by others (Schwall et al., 2000), but seems to appear only  
234 when starch granules are in contact with water as for preparation for light microscopy imaging.  
235 Using polarised light, starch granules display birefringence, shown as a Maltese cross (Figure 1  
236 D-F). This property indicates the radial order centred at the hilum, the growth centre of the  
237 granule, and is correlated with the orderly alignment of the starch molecules. There were some  
238 unevenly shaped granules in all three high-amylose starches displaying one or more overlapping  
239 crosses, but this was most obvious for HighAm-2012 containing the highest amount of amylose.

240 There was no loss of birefringence, indicating no major changes in the order and alignment of  
241 starch molecules within the granule. This is in contrast to previous studies producing high-  
242 amylose potato starches by inhibition of starch branching enzymes where starch granules of  
243 high-amylose lines displayed less birefringence (Schwall et al., 2000).

244 Besides the irregular shape, high-amylose lines exhibited granules with overlapping of two or  
245 more crosses. A theory has been proposed that the altered shape of the granules is a result of  
246 failed amyloplast separation and thus the division of the amyloplast is retarded during  
247 development because of the fusion of two granules by amylose interaction, forming helices  
248 (Jiang, Horner, Pepper, Blanco, Campbell & Jane, 2010). Hence, rod and triangular shaped  
249 granules are prevalent in potato starches with higher amylose content.

250



251  
 252 **Figure 1.** Light microscopy images of starch granules (A to C: stained with iodine, D to F: under  
 253 polarised light), photos of solution-cast films (G to I), SEM images of film surface (J to L) and

254 TEM images of microstructural network (M to O, arrows indicate pores) from high-amylose  
255 lines LowAm-1068, MidAm-7040 and HighAm-2012.

256

### 257 **3.2 Amylose content by colorimetry and gel permeation chromatography**

258 Amylose content was determined based on iodine complex formation. The amylose content was  
259 about 30% for the wild-type starches (Table 1), which was slightly higher than expected for  
260 common potato starches using iodine (Morrison & Laignelet, 1983). This could be due to an  
261 overestimation of amylose when using an extracted amylose standard for calibration which  
262 probably has a lower chain length than in native starches. As expected, the three high-amylose  
263 lines exhibited elevated amylose content, from 45-89%. The basis for colorimetric amylose  
264 determination is the property of amylose to form a colorful complex with iodine depending on  
265 the chain length of the polymer. No differentiation can be made on interference from color  
266 formation by long-chain amylopectin molecules with iodine to a complex, and hence the  
267 technique can give an overestimation of the amylose content (Morrison & Laignelet, 1983;  
268 Vilaplana, Hasjim & Gilbert, 2012).

269

270 **Table 1.** Tuber yield, dry matter of fresh weight, starch purity and amylose content of wild-type  
271 starches (Kuras, Verba, Dinamo) and their high-amylose lines (LowAm-1068, MidAm-7040,  
272 HighAm-2012) determined colorimetrically using iodine binding and by gel permeation  
273 chromatography (GPC) after debranching.

Sample	Tuber yield [%] <sup>a</sup>	Dry matter of fresh weight [%]	Starch purity [%] <sup>b</sup>	Amylose content [%]	
				Colorimetric <sup>c</sup>	GPC <sup>d</sup>

Kuras	100	31	86.3 ± 1.35	30 ± 0.3	22 ± 4.0
LowAm-1068	169	25	81.5 ± 0.88	45 ± 0.9	26 ± 0.8
Verba	100	31	87.9 ± 1.59	31 ± 1.9	23 ± 1.2
MidAm-7040	154	29	77.7 ± 2.23	70 ± 2.4	39 ± 0.8
Dinamo	100	31	85.3 ± 1.26	30 ± 0.8	23 ± 2.0
HighAm-2012	219	18	75.6 ± 2.76	89 ± 1.2	49 ± 5.8

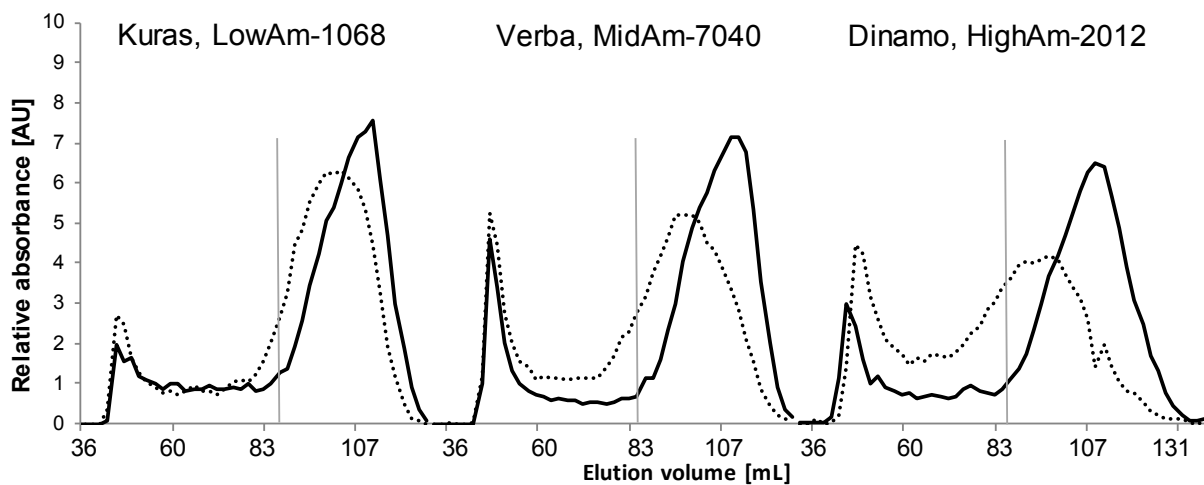
274 <sup>a</sup> relative to wild-type potato cultivar, <sup>b</sup> Starch content based on dry matter (mean ± stdev., n=3)  
 275 determined enzymatically according to Åman, Westerlund and Theander (1994), <sup>c</sup> based on  
 276 starch content (mean ± stdev., n=4), <sup>d</sup> mean and standard error

277 Molar mass distribution of intact starches was carried out on Sepharose CL-2B columns  
 278 (supplementary material) and showed a typical pattern of potato starch with two peaks  
 279 corresponding to amylopectin with a typical wavelength at maximum absorbance of 560 nm and  
 280 an amylose peak with a typical wavelength at maximum absorbance of about 640 nm.

281 Separation using GPC of debranched molecules can give a better estimate of amylose content. A  
 282 granular potato amylopectin starch standard was used to indicate the elution volume where the  
 283 first chains of debranched amylopectin elute from the column (at elution volume 85 mL;  
 284 Figure 2). In order to compare the starches, the amylose content was determined as the relative  
 285 area under the curve from 40 to 85 mL. The corresponding amylose content of the three wild-  
 286 type starches was about 23%, while their high-amylose lines LowAm-1068, MidAm-7040 and  
 287 HighAm-2012 contained about 26%, 39% and 49% of amylose, respectively. Not only was the  
 288 amount of amylose (first peak in chromatogram; Figure 2) increased, but the composition of  
 289 chain lengths in amylose and amylopectin changed, resulting in a shift in the chromatogram  
 290 (Figure 2, dotted lines). The elution profile of the debranched starches showed that with  
 291 increasing amylose content, the separation between the two components was less obvious. This

292 indicates that amylopectin molecules of the high-amylose line starches exhibited a higher amount  
293 of long chains and/or that amylose molecules were slightly branched. As discussed below, it was  
294 shown that amylopectin molecules had longer chains and that amylose molecules were not  
295 changed. This is in agreement with previous studies on genetically modified high-amylose potato  
296 starches, reporting an increase in average chain length in amylopectin (Blennow, Hansen,  
297 Schulz, Jørgensen, Donald & Sanderson, 2003; Hofvander, Andersson, Larsson & Larsson,  
298 2004; Schwall et al., 2000).

299  
300



301

302 **Figure 2.** Gel permeation chromatograms on Sepharose CL-6B of wild-type potato starches  
303 Kuras, Verba, Dinamo (solid line) and their high-amylose lines LowAm-1068, MidAm-7040,  
304 HighAm-2012 (dotted line) after debranching with isoamylase/ pullulanase. Gray vertical lines  
305 represent division of amylose and amylopectin for amylose content calculation, based on a  
306 standard of granular amylopectin potato starch.

307 Recently, there have been many efforts to define amylose content and validation of methods to  
308 determine amylose content (Vilaplana, Hasjim & Gilbert, 2012; Vilaplana, Meng, Hasjim &

309 Gilbert, 2014). However, with high-amylose starches with altered structure, the definition  
 310 becomes more complicated and it is well known that assays based on iodine binding can  
 311 overestimate amylose content (Cheetham & Tao, 1997; Hofvander, Andersson, Larsson &  
 312 Larsson, 2004; Schwall et al., 2000; Shi, Capitani, Trzasko & Jeffcoat, 1998; Vilaplana, Hasjim  
 313 & Gilbert, 2012). In a recent study by Vilaplana et al. (2014), two-dimensional distributions  
 314 based on molecular size and branch chain length revealed the complex topologies of high-  
 315 amylose maize starch showing the presence of distinct intermediate compounds with the  
 316 molecular size of amylose, but branching structure similar to that of amylopectin, albeit having  
 317 longer chain length (Vilaplana, Meng, Hasjim & Gilbert, 2014).

318

### 319 **3.3 Separation of amylose and amylopectin using n-butanol-amylose complex formation**

320 To study the changed structure of the high-amylose starches in more detail, amylopectin and  
 321 amylose were isolated through chemical fractionation using n-butanol. The purity of each  
 322 fraction was determined using GPC of debranched samples. All isolated amylopectin fractions of  
 323 wild-type starches showed  $\leq 3.5\%$  amylose and were hence considered pure (Table 2 and Figure  
 324 3). The amylopectin isolated from the high-amylose lines exhibited up to 18% amylose  
 325 (calculated at the same separation volume for division of the two components at 85 mL shown in  
 326 Figure 2).

327 **Table 2.** Yield and purity of amylose (AM) and amylopectin (AP) after separation with n-  
 328 ButOH/ iso-amylalcohol (1<sup>st</sup> separat.) and second separation of the amylose fraction (AM  
 329 separat.)

Sample	Yield after ButOH <sup>a</sup>	Purity <sup>b</sup>	
		1 <sup>st</sup> separat.	AM separat.

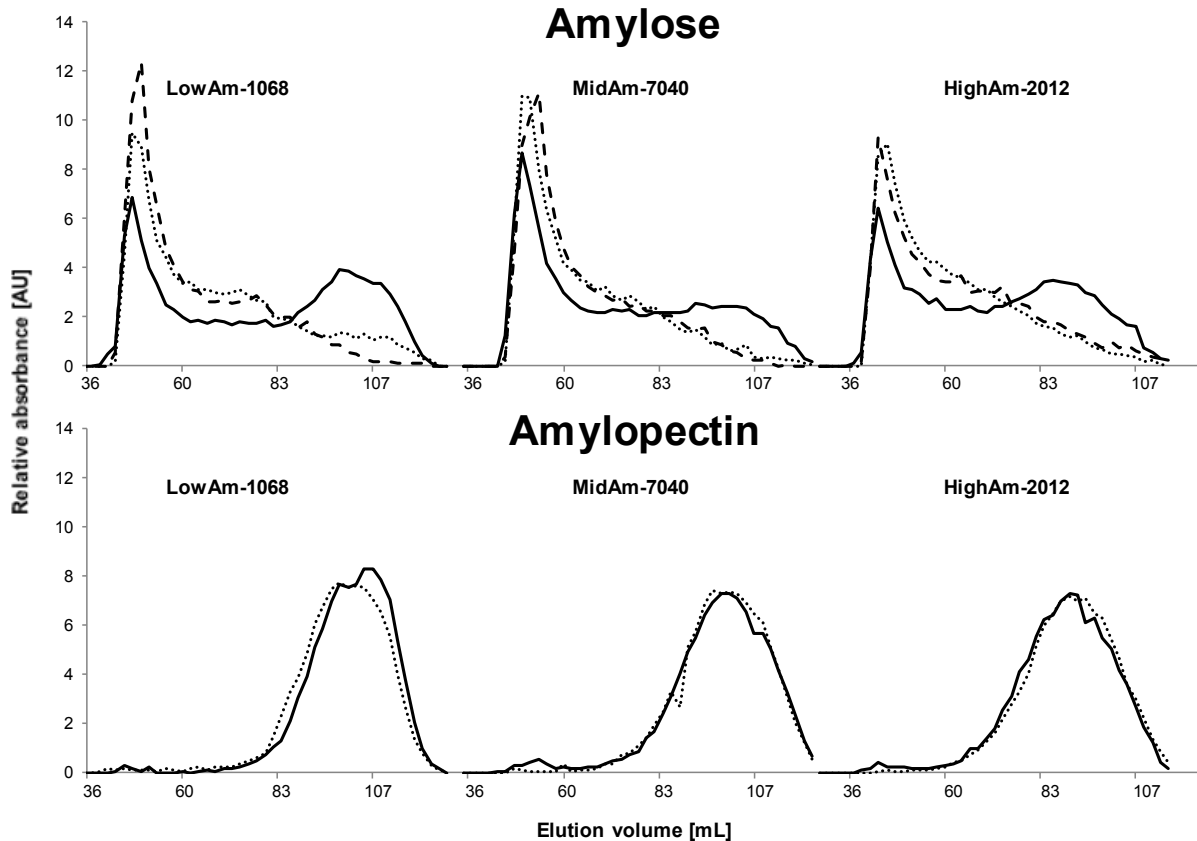
	1 <sup>st</sup> separat.	AM separat.	AP	AM	AP	AM
Kuras	91.9	54.1	97.9	62.9	93.3	91.4
LowAm-1068	87.5	31.3	95.6	52.2	93.7	78.2
Verba	96.3	62.4	96.5	65.3	97.5	92.8
MidAm-7040	97.5	55.0	88.2	66.7	89.3	86.5
Dinamo	79.5	51.3	98.7	62.7	96.2	75.3
HighAm-2012	102.0	26.7	81.6	59.1	85.0	84.7

330 <sup>a</sup> Yield in % calculated gravimetrically based on starch content (sum of amylose and amylopectin  
331 after n-butanol fractionation), <sup>b</sup> Determined in % using GPC on Sepharose CL-6B after  
332 debranching, point of division at 85 mL elution volume

333 However, the chromatograms showed that the amylopectin structure was changed compared to  
334 the wild-type starches, displaying an increased amount of longer chains rather than an impurity  
335 from amylose. Hence, the division between amylopectin and amylose was adjusted to be at  
336 elution volume 65 mL resulting in  $\geq 95\%$  purity of isolated amylopectin fractions (data not  
337 shown). Isolated amylose fractions were less pure and contained a considerable amount of  
338 amylopectin (Figure 3, solid line). Hence, those isolated amylose fractions were precipitated with  
339 n-butanol once more. The second isolate of amylose (Figure 3, dotted line) showed no  
340 amylopectin peak in the elution profile, but rather a long tailing amylose peak. Amylopectin  
341 isolated from the amylose fraction showed the same elution profile as amylopectin isolated from  
342 whole starch (Figure 3, dotted line) and hence was considered to reflect remnants from the  
343 separation. In order to distinguish whether only linear amylose, low-branched amylose or low-  
344  $M_w$  amylopectin with long-chains was present in the amylose fractions, the samples were run  
345 without debranching using GPC (Figure 3, dashed line). A change in the chromatogram would  
346 have indicated branching. However, it was found that all isolated amylose fractions consisted of  
347 linear chains. Similar results have been reported for high-amylose maize starches, i.e. low- $M_w$   
348 fractions were not branched, as debranching with isoamylase did not show any differences in the

349 gel permeation chromatogram (Shi, Capitani, Trzasko & Jeffcoat, 1998). A small difference was  
350 seen for the amylose fraction of LowAm-1068 (Figure 3, dashed line), where a minor peak  
351 probably indicated some impurity from amylopectin molecules.

352



353

354 **Figure 3.** Gel permeation chromatogram on Sepharose CL-6B after debranching of high-  
355 amylose potato lines LowAm-1068, MidAm-7040 and HighAm-2012: isolated amylose and  
356 amylopectin fractions (solid line = first separation, dotted line = second separation, dashed line =  
357 second separation without debranching).

358 The elution profiles of the isolated compounds demonstrated that there was little difference in the  
359 amylose fractions of the high-amylose lines, as reported elsewhere (Banks, Greenwood & Muir,  
360 1974). However, the amylopectin fraction showed a profile shift to longer chains. Hence, further

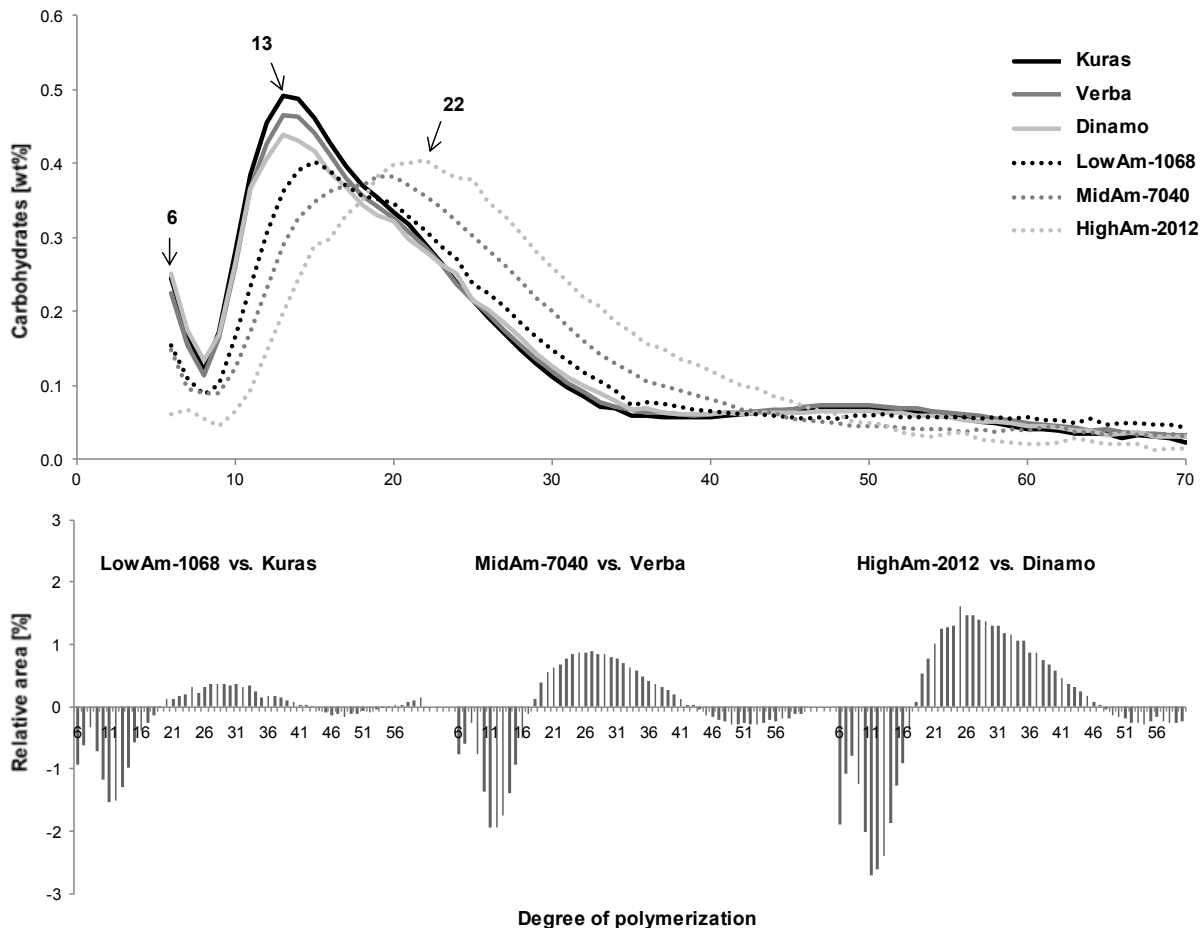
361 investigations on the chain length distribution were carried out and are discussed in more detail  
362 below.

363

### 364 3.4 Chain length distribution of amylopectin

365 Since the distribution and size of linear amylose molecules was considered to be similar in all  
366 three starches, no further investigations were carried out on these samples. Instead, amylopectin  
367 was investigated in more detail. Chain length distribution of isolated amylopectin was  
368 determined using HPAEC-PAD and the unit chain profiles were plotted (Figure 4).

369



370

371 **Figure 4.** Chain length distribution after debranching of amylopectin of wild-type starches

372 Kuras, Verba, Dinamo (solid line) and their high-amylose lines LowAm-1068, MidAm-7040,

373 HighAm-2012 (dotted line) using HPAEC-PAD and difference between the relative areas in the  
374 chain length distribution of high-amylose line minus wild-type starch (lower part).

375 The amylopectin average chain length of all wild-type starches was about 35, with a peak at  
376 degree of polymerization (DP) 13 (Figure 4). Similar profiles of regular potato amylopectin have  
377 been reported by others (Jane et al., 1999; Koch, Andersson & Åman, 1998). In contrast, molar  
378 proportions of chains with DP 18-37 increased in all high-amylose lines. The peak DP peak  
379 shifted to 22 for HighAm-2012. The changes in the individual unit chains between the  
380 amylopectin of wild-type starch and their corresponding high-amylose lines are visualized in the  
381 lower part of Figure 4. In the high-amylose lines, chains with DP 6-8 were particularly  
382 decreased. These chains have been shown to possess typical profiles depending on the crop and  
383 are probably outermost chains in the amylopectin (Bertoft, 2004). The proportion of short chains  
384 (DP 6-18) in amylopectin of HighAm-2012 was decreased by 50%, that of MidAm-7040 by at  
385 least 32% and that of LowAm-1068 by about 13% (Figure 4). More thorough investigations of  
386 the fine structure of amylopectin, i.e.  $\beta$ -limit and  $\phi, \beta$ -limit dextrin, would give a better  
387 understanding of which chain categories, outer and inner chains, are involved in the molecular  
388 network formation (Bertoft, 2007).

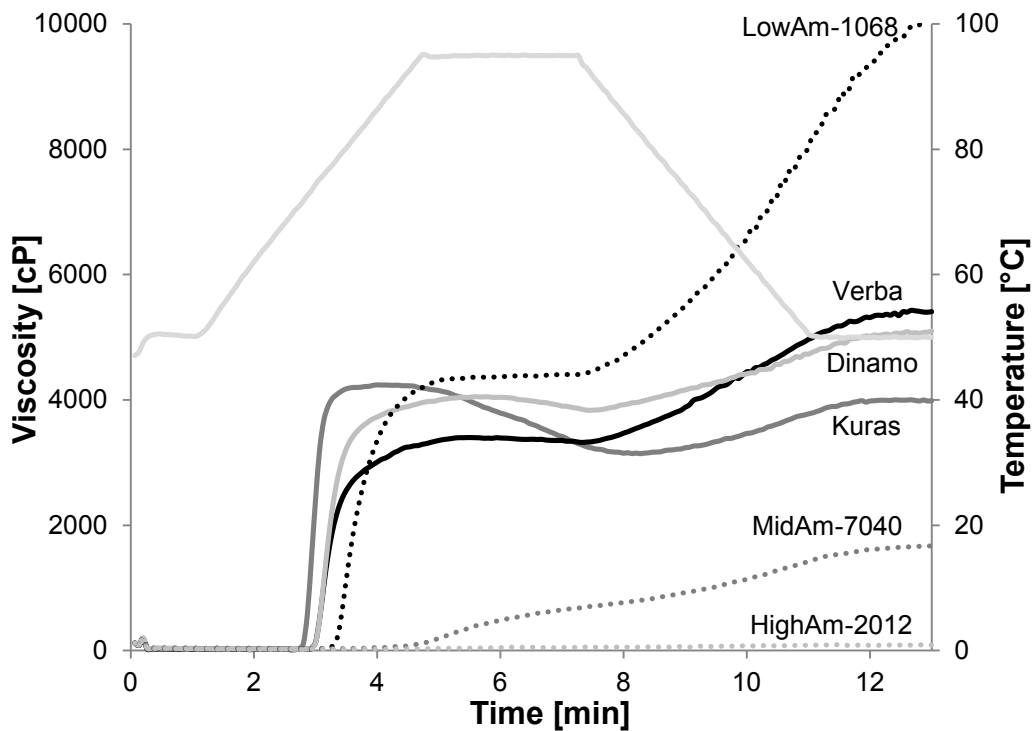
389

### 390 **3.5 Pasting properties of starches**

391 Starch pasting properties provide information on the ability to form a paste after heating and  
392 cooling. Native potato starch does not solubilize at temperatures lower than 50 °C, but when  
393 heated in water starch granules start absorbing water and swell. Wild-type potato starches started  
394 to swell at around 72-75 °C, seen as an increase in viscosity (Figure 5). As the temperature  
395 increases, starch granules rupture and more soluble amylose can leak out resulting in a small

396 decrease of the viscosity (breakdown). During the holding time, the material is subjected to high  
397 temperature and mechanical shear which further disrupted the granules. The holding strength is  
398 the ability of a material to withstand shear stress and heat, which was high in all wild-type potato  
399 starches. During the cooling phase, re-association of molecules, especially amylose, occurred in  
400 all wild-type starches resulting in the formation of a gel structure increasing viscosity (setback).  
401 The low setback region indicated a low rate of starch retrogradation. Even though there were  
402 differences in pasting behaviour between wild-type starches, our main focus was laid on the  
403 high-amylose starches. As seen from the RVA amylographs in Figure 4, there were large  
404 differences between the three high-amylose starches which showed a completely different profile  
405 compared to their wild-type counterparts.

406



407

408 **Figure 5.** Pasting profiles of wild-type starches Kuras, Verba, Dinamo (solid line) and their  
409 high-amylose lines LowAm-1068, MidAm-7040, HighAm-2012 (dotted line) measured using  
410 RVA. (Upper light grey line indicates temperature profile)

411 The high-amylose starch LowAm-1068 had a higher pasting temperature (79 °C) and final  
412 viscosity and a substantially higher setback compared to wild-type starches. The higher pasting  
413 temperature indicates a higher swelling capacity of granules. During the holding time, there was  
414 only a small breakdown detectable in LowAm-1068 which indicates that the material could  
415 withstand heat and shear forces and that not all granules were disrupted. Light microscopy  
416 images were taken after the RVA run (data not shown) and revealed a mixture of swollen  
417 granules and fragments of swollen granules within a continuous network. During cooling,  
418 viscosity increased with a final viscosity that was twice as high compared with wild-type  
419 starches, probably due to the slightly increased amylose content in LowAm-1068. Amylose re-  
420 associates during cooling until a gel structure is formed, which increases viscosity.

421 The two starches with highest amylose content showed very low or no granule swelling (Light  
422 microscopy images, data not shown) and viscosity (Figure 5) under the conditions used. It is  
423 primarily the amylopectin that is responsible for granule swelling, while the high amylose  
424 content alters the pasting properties and restricts swelling (Tester & Morrison, 1990). The  
425 inhibited granule swelling of starches with >55% amylose (colorimetric determination with  
426 iodine) has been reported previously (Karlsson, Leeman, Björck & Eliasson, 2007; Schwall et  
427 al., 2000).

428

429 **3.6 Microstructural characterization of solution-cast films**

430 As starches from high-amylose lines needed higher gelatinization temperatures, the starch water  
431 slurry was heated to 140 °C during vigorously stirring and then cast into Petri dishes. From the  
432 images of solution-cast films (Figure 1 G-I), it can be seen that film-formation was different for  
433 each high-amylose line. MidAm-7040 and HighAm-2012 gave cohesive but curled-up films;  
434 LowAm-1068 gave partly fragmented films. All three solution-cast films were homogeneous and  
435 no granule-shaped remnants or phase separation was seen (Light microscopy images, data not  
436 shown). The difference in film-formation of the three starches of the high-amylose lines could be  
437 due to the difference in amylose and amylopectin ratio as well as the difference in amylopectin  
438 structure (described below). Amylose is thought to be the better film-former resulting in cohesive  
439 films, whereas the higher amount of amylopectin in LowAm-1068 could result in the  
440 fragmentation of the film. It has been shown that high temperature and longer heating are  
441 necessary to completely disrupt starch granules of high-amylose starches (Bengtsson, Koch &  
442 Gatenholm, 2003; Koch, Gillgren, Stading & Andersson, 2010). On the other hand, harsh  
443 conditions could degrade amylose and amylopectin affecting the film cohesiveness negatively  
444 (Koch, Gillgren, Stading & Andersson, 2010). However, we did not expect a severe degradation  
445 of starch during heating to 140 °C as in the study of Koch et al. (2010) 150 °C were needed to  
446 significantly degrade starch. There is little known about time and temperature conditions to  
447 produce homogenous solution cast films (Koch, Gillgren, Stading & Andersson, 2010) and the  
448 effect on molecular structure, microstructure and material properties. Hence, further  
449 investigations are required. A general problem is that most studies are not explicit on the  
450 conditions to solubilize starch to produce solution cast films; i.e. in this study it took 45 min to  
451 heat up the sample tube to the holding temperature of 140 °C.

452

453 SEM images have shown a more uneven surface texture for films of starches with higher  
454 amylose content (Figure 1 J-L). Similar findings have previously been attributed to remnants of  
455 granules after gelatinization and/or fast aggregation of amylose during the cooling process,  
456 resulting in a rougher surface (Bengtsson, Koch & Gatenholm, 2003; Koch, Gillgren, Stading &  
457 Andersson, 2010). However, in our study, light microscopy images (iodine staining and  
458 differential interference contrast) did not reveal any granule-shaped remnants.

459 The microstructure of solution-cast films was studied using TEM. TEM micrographs (Figure 1  
460 M-O) showed mainly darkly stained starch molecules and brighter pore areas (indicated by  
461 arrows). Since individual amylopectin molecules are different from amylose molecules in size  
462 and structure and vary between the high-amylose lines, the TEM-images were expected to show  
463 morphological differences. At first sight, all films looked similar showing a rather homogenous  
464 and dense structure. However, there were distinct differences between films regarding pore size  
465 and shape. TEM micrographs of LowAm-1068 films (Figure 1 M) revealed small pores  
466 (indicated by arrows) of about 10 nm (through a few manual measurements) which were mainly  
467 round-shaped and representing an amylopectin-like branched network structure (Leloup,  
468 Colonna, Ring, Roberts & Wells, 1992). TEM micrographs of MidAm-7040 films showed a  
469 more heterogeneous pore distribution with less regular shaped pores up to 30-40 nm in size.  
470 HighAm-2012 films exhibited a more open but also fractal-structure with pore sizes up to 60 nm  
471 which could be argued to be more amylose-like and revealing some rod-like strands. TEM  
472 micrographs of the films LowAm-1068 and MidAm-7040 did not evidently reveal the dense  
473 amylose-like structure as reported previously for pure amylose gels and films (Leloup, Colonna,  
474 Ring, Roberts & Wells, 1992; Richardson, Kidman, Langton & Hermansson, 2004; Rindlav-  
475 Westling, Stading, Hermansson & Gatenholm, 1998). The morphology of the HighAm-2012

476 film, however, showed some indication of a more open structure with stiff rod-like strands and  
477 was more alike pure amylose gels and films. As discussed above, the genetic modification of the  
478 potato resulted in a change in amylopectin structure besides an increase in amylose content  
479 (Figure 2). We therefore suggest that not only amylose but also long chains of amylopectin or  
480 intermediate components can contribute to the change in microstructure, e.g. physical  
481 entanglements between longer branches and amylose chains, observed using TEM. However,  
482 further investigations are needed to better understand the created starch network structure seen in  
483 TEM images.

484

### 485 **3.7 Barrier properties and tensile strength of solution-cast films**

486 Oxygen permeability (OP) was studied in solution-cast films of all three high-amylose lines and  
487 compared with the wild-type Dinamo (Table 3). It was found that all three high-amylose lines  
488 exhibited lower OP ( $P < 0.01$ ) than native potato starch films. In addition, OP was much lower  
489 than in materials made from most synthetic polymers. In a previous study on amylose films,  
490 better barrier properties were attributed to higher crystallinity compared with amylopectin films  
491 (Rindlav-Westling, Stading, Hermansson & Gatenholm, 1998). This would decrease the  
492 solubility of oxygen, resulting in a lower oxygen transmission rate.

493 Starch films of the high-amylose lines exhibited higher stress at break compared with the wild-  
494 type starch film Dinamo (Table 3;  $P < 0.05$ ). The stiffness and higher strength of these films  
495 compared with wild-type starch could be attributable to the longer chains in amylopectin being  
496 involved in the interconnected network and increasing the interaction between chains.  
497 Furthermore, strain at break increased in all high-amylose lines (Table 3;  $P < 0.05$ ). It has been  
498 shown previously for starch films of different amylose and amylopectin mixtures that higher  
499 amylose content increases elongation (Lourdin, Valle & Colonna, 1995). As compared to

500 commonly used oxygen barriers, such as EVOH (poly ethylene-co-vinylalcohol), the stress at  
 501 break is considerable higher but the strain at break is lower when measured at the same  
 502 conditions (23 °C and 50% RH). The high standard deviations are due to the strong polar bonds  
 503 and a high surface energy. This facilitates fracture propagation from, e.g. a small flaw in the  
 504 surface, as easily introduced when cutting the samples for the tensile test. The standard deviation  
 505 decreases when testing hundreds of samples, but the interesting effect of such materials is that  
 506 they may facilitate easy-to-open packages. However, the films or coatings in a real package  
 507 would be supported by a water barrier and sealant layer of, e.g. renewable polyethylene that also  
 508 would give the main contribution to the mechanical properties of the package.  
 509

510 **Table 3.** Oxygen permeability (OP), stress at break and strain at break of parental starch Dinamo  
 511 and high-amylose lines, high-amylose maize starch, low-density polyethylene (LDPE) and poly  
 512 ethylene-co-vinylalcohol (EVOH)

Sample	OP <sup>a</sup> [cc mm/ m <sup>2</sup> 24h atm]	Stress at break <sup>b</sup> [MPa]	Strain at break <sup>b</sup> [%]
Dinamo	0.170 ± 0.01	34.1 ± 9.5	1.5 ± 0.3
LowAm-1068	0.089 ± 0.04	42.2 ± 3.7	2.8 ± 0.4
MidAm-7040	0.100 ± 0.03	45.0 ± 12.0	2.3 ± 0.8
HighAm-2012	0.085 ± 0.03	46.0 ± 12.4	3.4 ± 2.2
High-amylose maize starch <sup>c</sup>		40	1.9
LDPE <sup>d</sup>	1900	7-16	100-800
EVOH <sup>e</sup>	0.01-12	20-210	20-330

513 <sup>a</sup> mean ± standard error (n=2), <sup>b</sup> mean ± standard deviation (n=6), moisture content was between  
514 10.2 to 10.4 % in the starch films, <sup>c</sup> from Koch, Gillgren, Stading and Andersson (2010), <sup>d</sup> from  
515 Doak (1986), <sup>e</sup> from Lange and Wyser (2003)

516

#### 517 **4. Conclusions**

518 Targeted gene suppression of *SBE1* and *SBE2* through RNA interference in three different potato  
519 cultivars resulted in high-amylose starches, which were characterized in detail and used to relate  
520 film performance to molecular structure. These high-amylose lines revealed starches with  
521 changed granular and molecular structures, pasting properties and film performance. The  
522 amylose content was increased to 45, 70 and 89% using iodine binding-based measurements.  
523 However, GPC revealed a more reliable amylose content of 26, 39 and 49% as the chain length  
524 of amylopectin was increased in addition to amylose content affecting the measurement when  
525 using the colorimetric method. The genetic modification produced starches with increasing  
526 amount of irregular shaped granules yielding basically no pasting at 95 °C. At high temperature,  
527 140 °C, all three starches were gelatinized. Highest amylose content and amylopectin with the  
528 longest chains resulted in cohesive films with a rough surface and improved physical properties.  
529 The improved oxygen barrier provided by the starches from high-amylose potato and their  
530 superior mechanical properties in terms of stronger films and increased strain at break indicate  
531 that they have the potential for interesting commercial applications such as in films or coatings.  
532 They are thought to have a particularly interesting future as barrier coatings, as the presently  
533 used industrial facilities (e.g. blade and curtain coaters) possibly could be used when applying  
534 them on boards or polymer films. However, they may have the same shortcomings as poor water  
535 barriers and must, just like the currently used oxygen barrier polymers, be encapsulated between  
536 two hydrophobic layers, that could for example be renewable polyethylene and tie layers.

537

538 **Acknowledgement**

539 Financial support from the project Trees and Crops for the Future, Mistra Biotech and SLU mat  
540 is gratefully acknowledged. We would like to thank Kristina Junel for technical assistance with  
541 OTR measurements and Ann-Sofie Fält for technical assistance with regeneration and growth of  
542 the plants.

543 **References**

- 544 Andersson, M., Melander, M., Pojmark, P., Larsson, H., Bulow, L., & Hofvander, P. (2006).  
545 Targeted gene suppression by RNA interference: An efficient method for production of high-  
546 amylose potato lines. *Journal of Biotechnology*, 123(2), 137-148.
- 547 Andersson, M., Trifonova, A., Andersson, A. B., Johansson, M., Bulow, L., & Hofvander, P.  
548 (2003). A novel selection system for potato transformation using a mutated AHAS gene. *Plant*  
549 *Cell Reports*, 22(4), 261-267.
- 550 Banks, W., Greenwood, C. T., & Muir, D. D. (1974). Studies on Starches of High Amylose  
551 Content. Part 17. A Review of Current Concepts. *Starch - Stärke*, 26(9), 289-300.
- 552 Bengtsson, M., Koch, K., & Gatenholm, P. (2003). Surface octanoylation of high-amylose potato  
553 starch films. *Carbohydrate Polymers*, 54(1), 1-11.
- 554 Bertoft, E. (2004). On the nature of categories of chains in amylopectin and their connection to  
555 the super helix model. *Carbohydrate Polymers*, 57(2), 211-224.
- 556 Bertoft, E. (2007). Composition of clusters and their arrangement in potato amylopectin.  
557 *Carbohydrate Polymers*, 68(3), 433-446.
- 558 Bertoft, E., & Spoof, L. (1989). Fractional precipitation of amylopectin alpha-dextrins using  
559 methanol. *Carbohydrate Research*, 189(0), 169-180.
- 560 Blennow, A., Hansen, M., Schulz, A., Jørgensen, K., Donald, A. M., & Sanderson, J. (2003). The  
561 molecular deposition of transgenically modified starch in the starch granule as imaged by  
562 functional microscopy. *Journal of Structural Biology*, 143(3), 229-241.
- 563 Cheetham, N. W. H., & Tao, L. (1997). The effects of amylose content on the molecular size of  
564 amylose, and on the distribution of amylopectin chain length in maize starches. *Carbohydrate*  
565 *Polymers*, 33(4), 251-261.
- 566 Chrastil, J. (1987). Improved colorimetric determination of amylose in starches or flours.  
567 *Carbohydrate Research*, 159(1), 154-158.
- 568 Doak, K. W. (1986). *Ethylene polymers*. Encyclopedia of polymer science and engineering: In J.I.  
569 Kroschwitz et al. (Eds.).
- 570 DuBois, M., Gilles, K. A., Hamilton, J. K., Rebers, P. A., & Smith, F. (1956). Colorimetric  
571 Method for Determination of Sugars and Related Substances. *Analytical Chemistry*, 28(3), 350-  
572 356.
- 573 Feng, Q., Hu, F., & Qiu, L. (2013). Microstructure and characteristics of high-amylose corn  
574 starch–chitosan film as affected by composition. *Food Science and Technology International*,  
575 19(3), 279-287.
- 576 Hofvander, P., Andersson, M., Larsson, C.-T., & Larsson, H. (2004). Field performance and  
577 starch characteristics of high-amylose potatoes obtained by antisense gene targeting of two  
578 branching enzymes. *Plant Biotechnology Journal*, 2(4), 311-320.
- 579 Jane, J., Chen, Y. Y., Lee, L. F., McPherson, A. E., Wong, K. S., Radosavljevic, M., &  
580 Kasemsuwan, T. (1999). Effects of Amylopectin Branch Chain Length and Amylose Content on  
581 the Gelatinization and Pasting Properties of Starch1. *Cereal Chemistry Journal*, 76(5), 629-637.
- 582 Jiang, H., Horner, H. T., Pepper, T. M., Blanco, M., Campbell, M., & Jane, J.-I. (2010).  
583 Formation of elongated starch granules in high-amylose maize. *Carbohydrate Polymers*, 80(2),  
584 533-538.
- 585 Karimi, M., Inze, D., & Depicker, A. (2002). GATEWAY(TM) vectors for Agrobacterium-  
586 mediated plant transformation. *Trends in Plant Science*, 7(5), 193-195.

587 Karlsson, M. E., Leeman, A. M., Björck, I. M. E., & Eliasson, A.-C. (2007). Some physical and  
588 nutritional characteristics of genetically modified potatoes varying in amylose/amylopectin  
589 ratios. *Food Chemistry*, *100*(1), 136-146.

590 Klucinec, J. D., & Thompson, D. B. (1998). Fractionation of High-Amylose Maize Starches by  
591 Differential Alcohol Precipitation and Chromatography of the Fractions. *Cereal Chemistry*  
592 *Journal*, *75*(6), 887-896.

593 Koch, K., Andersson, R., & Åman, P. (1998). Quantitative analysis of amylopectin unit chains  
594 by means of high-performance anion-exchange chromatography with pulsed amperometric  
595 detection. *Journal of Chromatography A*, *800*(2), 199-206.

596 Koch, K., Gillgren, T., Stading, M., & Andersson, R. (2010). Mechanical and structural  
597 properties of solution-cast high-amylose maize starch films. *International Journal of Biological*  
598 *Macromolecules*, *46*(1), 13-19.

599 Lange, J., & Wyser, Y. (2003). Recent innovations in barrier technologies for plastic  
600 packaging—a review. *Packaging Technology and Science*, *16*(4), 149-158.

601 Larsson, C. T., Hofvander, P., Khoshnoodi, J., Ek, B., Rask, L., & Larsson, H. (1996). Three  
602 isoforms of starch synthase and two isoforms of branching enzyme are present in potato tuber  
603 starch. *Plant Science*, *117*(1-2), 9-16.

604 Leloup, V. M., Colonna, P., Ring, S. G., Roberts, K., & Wells, B. (1992). Microstructure of  
605 amylose gels. *Carbohydrate Polymers*, *18*(3), 189-197.

606 Li, M., Liu, P., Zou, W., Yu, L., Xie, F., Pu, H., Liu, H., & Chen, L. (2011). Extrusion  
607 processing and characterization of edible starch films with different amylose contents. *Journal of*  
608 *Food Engineering*, *106*(1), 95-101.

609 Liu, Z. (2005). Edible films and coatings from starches. In H. H. Jung (Ed.). *Innovations in Food*  
610 *Packaging* (pp. 501-513). London: Academic Press.

611 Lourdin, D., Valle, G. D., & Colonna, P. (1995). Influence of amylose content on starch films  
612 and foams. *Carbohydrate Polymers*, *27*(4), 261-270.

613 Morrison, W. R., & Laignelet, B. (1983). An improved colorimetric procedure for determining  
614 apparent and total amylose in cereal and other starches. *Journal of Cereal Science*, *1*(1), 9-20.

615 Muscat, D., Adhikari, B., Adhikari, R., & Chaudhary, D. S. (2012). Comparative study of film  
616 forming behaviour of low and high amylose starches using glycerol and xylitol as plasticizers.  
617 *Journal of Food Engineering*, *109*(2), 189-201.

618 Muscat, D., Adhikari, R., McKnight, S., Guo, Q., & Adhikari, B. (2013). The physicochemical  
619 characteristics and hydrophobicity of high amylose starch–glycerol films in the presence of three  
620 natural waxes. *Journal of Food Engineering*, *119*(2), 205-219.

621 Myllarinen, P., Partanen, R., Seppala, J., & Forssell, P. (2002). Effect of glycerol on behaviour  
622 of amylose and amylopectin films. *Carbohydrate Polymers*, *50*(4), 355-361.

623 Rankin, J. C., Wolff, I. A., Davis, H. A., & Rist, C. E. (1958). Permeability of amylose film to  
624 moisture vapor, selected organic vapors, and the common gases. *Journal of Chemical and*  
625 *Engineering Data*, *3*(1), 120-123.

626 Richardson, G., Kidman, S., Langton, M., & Hermansson, A.-M. (2004). Differences in amylose  
627 aggregation and starch gel formation with emulsifiers. *Carbohydrate Polymers*, *58*(1), 7-13.

628 Richardson, P. H., Jeffcoat, R., & Shi, Y.-C. (2000). High-Amylose Starches: From Biosynthesis  
629 to Their Use as Food Ingredients. *MRS Bulletin*, *25*(12), 20-24.

630 Rindlav-Westling, Å., Stading, M., & Gatenholm, P. (2001). Crystallinity and Morphology in  
631 Films of Starch, Amylose and Amylopectin Blends. *Biomacromolecules*, *3*(1), 84-91.

632 Rindlav-Westling, Å., Stading, M., Hermansson, A.-M., & Gatenholm, P. (1998). Structure,  
633 mechanical and barrier properties of amylose and amylopectin films. *Carbohydrate Polymers*,  
634 36(2-3), 217-224.

635 Schwall, G. P., Safford, R., Westcott, R. J., Jeffcoat, R., Tayal, A., Shi, Y.-C., Gidley, M. J., &  
636 Jobling, S. A. (2000). Production of very-high-amylose potato starch by inhibition of SBE A and  
637 B. *Nat Biotech*, 18(5), 551-554.

638 Shi, Y.-C., Capitani, T., Trzasko, P., & Jeffcoat, R. (1998). Molecular Structure of a Low-  
639 Amylopectin Starch and Other High-Amylose Maize Starches. *Journal of Cereal Science*, 27(3),  
640 289-299.

641 Sidebottom, C., Kirkland, M., Strongitharm, B., & Jeffcoat, R. (1998). Characterization of the  
642 Difference of Starch Branching Enzyme Activities in Normal and Low-Amylopectin Maize  
643 during Kernel Development. *Journal of Cereal Science*, 27(3), 279-287.

644 Tester, R. F., & Morrison, W. R. (1990). Swelling and gelatinization of cereal starches. I. Effects  
645 of amylopectin, amylose, and lipids. *Cereal Chemistry*, 67(6), 551-557.

646 Thiéry, J. P. (1967). Mise en évidence des polysaccharides sur coupes fines en  
647 microscopieelectronique. *Journal de Microscopie*(6), 987-1018.

648 Walker, J. T., & Merritt, N. R. (1969). Genetic Control of Abnormal Starch Granules and High  
649 Amylose Content in a Mutant of Glacier Barley. *Nature*, 221(5179), 482-483.

650 Van Patten, E. M., & Freck, J. A. (1973). Method of coating food products with ungelatinized  
651 unmodified high amylose starch prior to deep fat frying. Google Patents.

652 Vilaplana, F., Hasjim, J., & Gilbert, R. G. (2012). Amylose content in starches: Toward optimal  
653 definition and validating experimental methods. *Carbohydrate Polymers*, 88(1), 103-111.

654 Vilaplana, F., Meng, D., Hasjim, J., & Gilbert, R. G. (2014). Two-dimensional macromolecular  
655 distributions reveal detailed architectural features in high-amylose starches. *Carbohydrate*  
656 *Polymers*, 113(0), 539-551.

657 Wolff, I. A., Davis, H. A., Cluskey, J. E., Gundrum, L. J., & Rist, C. E. (1951). Preparation of  
658 Films from Amylose. *Industrial & Engineering Chemistry*, 43(4), 915-919.

659 Wolff, I. A., Hofreiter, B. T., Watson, P. R., Deatherage, W. L., & MacMasters, M. M. (1955).  
660 The Structure of a New Starch of High Amylose Content. *Journal of the American Chemical*  
661 *Society*, 77(6), 1654-1659.

662 Zeeman, S. C., Kossmann, J., & Smith, A. M. (2010). Starch: Its Metabolism, Evolution, and  
663 Biotechnological Modification in Plants. *Annual Review of Plant Biology*, Vol 61, 61, 209-234.

664 Åman, P., Westerlund, E., & Theander, O. (1994). Determination of starch using thermostable  $\alpha$ -  
665 amylase. *J.N. BeMiller, D.J. Manners, R.J. Sturgeon (Eds.), Methods in Carbohydrate*  
666 *Chemistry*, X(Wiley, New York), 111-115.

667

668